Separation Science and Technology
Publication details, including instructions for authors and subscription information:
http://www.informaworld.com/smpp/title~content=t713708471

Hydrotalcite Materials for Carbon Dioxide Adsorption at High Temperatures: Characterization and Diffusivity Measurements

José L. Soares[a]; Regina F. P. M. Moreira[a]; Humberto J. José[a]; Carlos A. Grande[b]; Alírio E. Rodrigues[b]
[a] Laboratório de Desenvolvimento de Processos Tecnológicos, Departamento de Engenharia Química e Engenharia de Alimentos, Universidade Federal de Santa Catarina, Florianópolis, SC, Brazil [b] Laboratory of Separation and Reaction Engineering, Departamento de Engenharia Química, Faculdade de Engenharia da Universidade do Porto, Porto, Portugal

Online publication date: 08 July 2010

To cite this Article Soares, José L. , Moreira, Regina F. P. M. , José, Humberto J. , Grande, Carlos A. and Rodrigues, Alírio E.(2005) 'Hydrotalcite Materials for Carbon Dioxide Adsorption at High Temperatures: Characterization and Diffusivity Measurements', Separation Science and Technology, 39: 9, 1989 — 2010
To link to this Article: DOI: 10.1081/SS-120039307
URL: http://dx.doi.org/10.1081/SS-120039307

SEPARATION SCIENCE AND TECHNOLOGY
Vol. 39, No. 9, pp. 1989–2010, 2004

Hydrotalcite Materials for Carbon Dioxide Adsorption at High Temperatures: Characterization and Diffusivity Measurements

José L. Soares,[1] Regina F. P. M. Moreira,[1,*] Humberto J. José,[1] Carlos A. Grande,[2] and Alírio E. Rodrigues[2]

[1]Laboratório de Desenvolvimento de Processos Tecnológicos, Departamento de Engenharia Química e Engenharia de Alimentos, Universidade Federal de Santa Catarina, Florianópolis, SC, Brazil
[2]Laboratory of Separation and Reaction Engineering, Departamento de Engenharia Química, Faculdade de Engenharia da Universidade do Porto, Porto, Portugal

ABSTRACT

Hydrotalcites are receiving considerable attention as adsorbents, catalysts, and catalyst precursors. However, the use of hydrotalcites as an

*Correspondence: Regina F. P. M. Moreira, Laboratório de Desenvolvimento de Processos Tecnológicos, Departamento de Engenharia Química e Engenharia de Alimentos, Universidade Federal de Santa Catarina, Florianópolis, SC, Brazil; E-mail: regina@enq.ufsc.br.

DOI: 10.1081/SS-120039307 0149-6395 (Print); 1520-5754 (Online)

adsorbent material for carbon dioxide has only been considered recently. In this work, three commercial hydrotalcites, Puralox MG30, MG50, and MG70, were used for the removal of CO_2 at temperatures in the range 423–623 K. The adsorbent materials were characterized by use of scanning electron microscopy/energy dispersive x-ray, mercury porosimetry, and N_2 adsorption at 77 K, which indicated the presence of micropores. The HK plot suggested pore-width values around 0.55 nm. The BET surface areas were 199, 154, and 144 m^2/g for MG30, MG50, and MG70, respectively. The micropore areas calculated by the DR method were 206, 161, and 146 m^2/g. The diffusivity of CO_2 onto hydrotalcite adsorbents was measured by the zero length column method. Kinetic studies indicated that the controlling mechanism for mass transfer inside the extrudate was micropore diffusion. The reciprocal of the time constants for micropore diffusion (D_c/l^2) were 8.5×10^{-3}–$15.3 \times 10^{-3}\,s^{-1}$ for MG30, 8.0×10^{-3}–$10.4 \times 10^{-3}\,s^{-1}$ for MG50, and 6.8×10^{-3}–$11.3 \times 10^{-3}\,s^{-1}$ for MG70, in the temperature range 423–623 K.

Key Words: Adsorption; Carbon dioxide; Hydrotalcite; ZLC.

INTRODUCTION

The removal and recovery of CO_2 from hot gas streams is becoming increasingly significant in the field of energy production. Large volumes of CO_2 are released to the environment by the combustion of fossil fuels, such as coal or natural gas, and this has become one of the most serious global environmental problems.[1] Typical flue gases contain about 17% CO_2, the balance being N_2 (79%) and O_2 (4%). Trace amounts of SO_2 and NO_x also can be found, but they are usually less than 1% in total.[2] The purification of flue gas by adsorption can play a key role in solving this problem.

The first step in any adsorption process is to find an appropriate adsorbent that is selective for CO_2. Carbon molecular sieves and zeolites have proved to be suitable adsorbents at low temperatures, but the capacity of adsorption is low at high temperature;[3,4] moreover, the adsorption of CO_2 on a carbon molecular sieve is not reversible, the adsorbent is partially oxidized, and its adsorption capacity is lost after several adsorption cycles.[3]

It has been reported that hydrotalcite is a more suitable adsorbent of CO_2, especially at high temperatures. Hydrotalcites belong to a large class of anionic clays that present layers of positively charged metallic oxide (or metallic hydroxide) with interlayers of anions, such as carbonates.

Such a structure enables this material to have adsorptive properties and stability under conditions of humidity and high temperature. Hydrotalcites can be represented by the general formula $[(M^{2+}_{1-x}\ M^{3+}_{x}\ (OH))^{x+}(A^{n-}_{x/n} \cdot mH_2O)^{x-}]$, where $M^{2+} = Mg^{2+}$, Ni^{2+}, Zn^{2+}, Cu^{2+}, Mn^{2+}; $M^{3+} = Al^{3+}$, Fe^{3+}, Cr^{3+}; $A^{n-} = CO_3^{2-}$, SO_4^{2-}, NO_3^-, Cl^-, OH^-, x is normally between 0.17 and 0.33. These materials have received considerable attention in recent years because they have a wide range of applications, mainly as catalysts and catalyst precursors.[5–7] Hydrotalcites have been studied by Yong et al.[1] and Ding and Alpay[8,9] for CO_2 adsorption in relation to a separation-enhanced reaction process for methane steam reforming.

Many experimental techniques have been developed with the goal of minimizing the effects of extraneous transport steps in diffusivity measurements. These include concentration pulse chromatography, the zero length column (ZLC) method,[10] pulsed field gradient nuclear magnetic resonance, quasi-elastic neutron scattering, uptake curves by microgravimetric technique, frequency response, and membrane techniques.[4]

The technique for measuring diffusivities by the ZLC method was first introduced by Eic and Ruthven in 1988.[11] This technique has been widely used to study both micropore and macropore diffusion as well as to follow exchange counter-diffusion in liquid-phase adsorption and tracer exchange in vapor systems.[12] Recent studies for the adsorptive separation of propane and propylene have used the ZLC technique to elucidate the controlling mass transfer mechanism.[13–16] Ruthven and Xu[17] also have used the ZLC method in the difficult separation of nitrogen and oxygen, and they have confirmed macropore control in 5A zeolites.

Traditionally, two methods have been used to analyze experimental data from the ZLC technique: the long-time (LT) and the short-time (ST) methods.[11] In the present study, the LT method was used where smaller experimental error was observed in comparison with the ST method. Recently, another method has been suggested by Han et al.[18] by using the entire information in the desorption curve. Silva and Rodrigues[15] have analyzed diffusivity measurements in bidisperse porous adsorbent pellets by the ZLC technique, and Brandani[19] has proposed an analytical solution for ZLC desorption curves with bi-porous adsorbent particles.

This paper is aimed at the characterization of three commercial hydrotalcite materials (Puralox MG30, MG50, and MG70 from Condea Chemie Gmbh, Germany) and the measurement of diffusivity and adsorption of CO_2 in cylindrical pellets (extrudates) of these adsorbents. The ZLC technique was used, because it eliminates extraneous mass-transfer limitations[11] and requires only a small sample of adsorbent.

CHARACTERIZATION OF THE HYDROTALCITE MATERIALS

The characterization of Puralox adsorbents was performed by scanning electron microscopy/energy dispersive x-ray (SEM/EDAX), mercury porosimetry, and N_2 adsorption at 77 K.

SEM/EDAX was performed with a JEOL JSM 6301F. Elemental microprobe and elemental distribution mapping techniques were used to analyze the composition of solid samples. Figure 1 shows that the extrudates were formed under pressure without the presence of a binder, and the adsorbent is highly porous with lamellar structures. The chemical composition of the samples is shown in Fig. 2.

The main characteristics of the three commercial hydrotalcites are that they have nearly the same surface area and different $MgO : Al_2O_3$ ratios. It has been reported that the aluminum content in hydrotalcites strongly affects the adsorption capacity of CO_2, since the density of the layer charge increases with the aluminum content, and this is favorable for adsorption of CO_2.[1,22] On the other hand, as the aluminum content increases, the interlayer spacing of the hydrotalcites decreases as the aluminum content increases, reducing the number of high strength CO_2 sites.[22,23] Therefore, there should be an optimum aluminum content in hydrotalcites for adsorption of CO_2.

Mercury porosimetry was performed with a Micromeritics Poresizer 9320 able to reach 30,000 psia. The mercury volume was measured during the intrusion and extrusion. The pore size distribution for MG50 is shown in Fig. 3. It may be observed that the adsorbents have high macroporosity.

The adsorption of N_2 at 77 K was performed with an Autosorb-1 (AS1 Chemisorb, Quantachrome, Germany). The adsorption isotherms [Fig. 4(A)–(C)] are type II of IUPAC classification.[20] The hysteresis indicates the presence of slit pores. The analysis of the N_2 adsorbed at $P/P_0 < 0.01$ was made according to the Horváth–Kawazoe method,[21] and the results are shown in Fig. 5. The micropore sizes are in the range 0.4–2.0 nm with a predominance of 0.55-nm pore width.

EXPERIMENTAL SECTION

Diffusivity Measurement of CO_2 onto Hydrotalcites

The diffusivity of CO_2 onto Puralox MG30, MG50, and MG70 was measured by using the ZLC method. Figure 6 shows the scheme of the experimental apparatus.

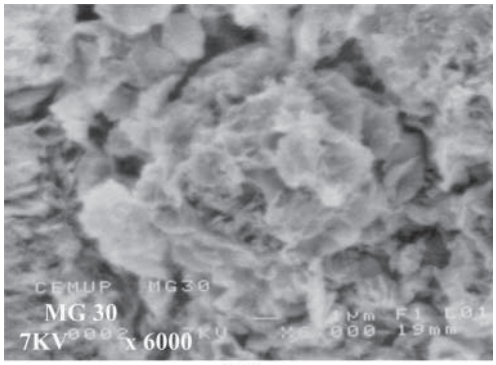

(A)

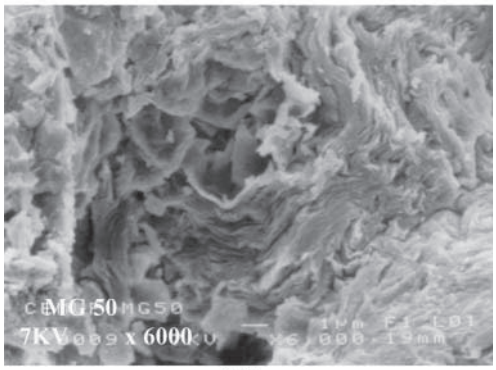

(B)

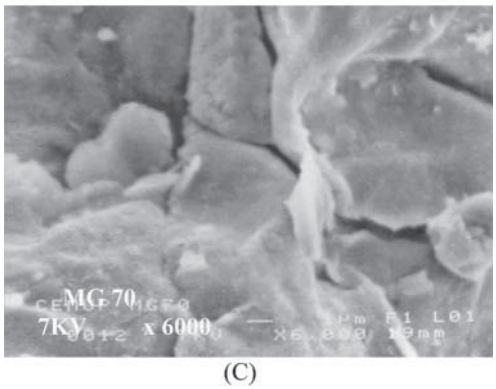

(C)

Figure 1. SEM for (A) MG30; (B) MG50; (C) MG70 (×6000).

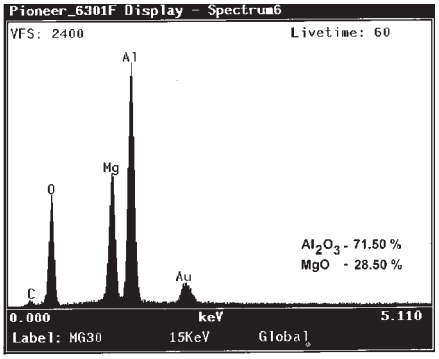

(A)

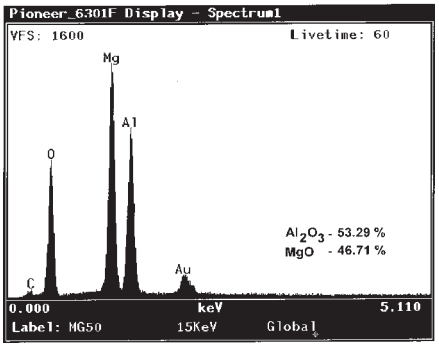

(B)

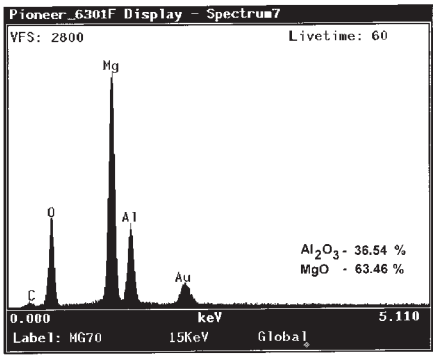

(C)

Figure 2. Chemical composition of (A) MG30; (B) MG50; and (C) MG70 obtained by EDAX.

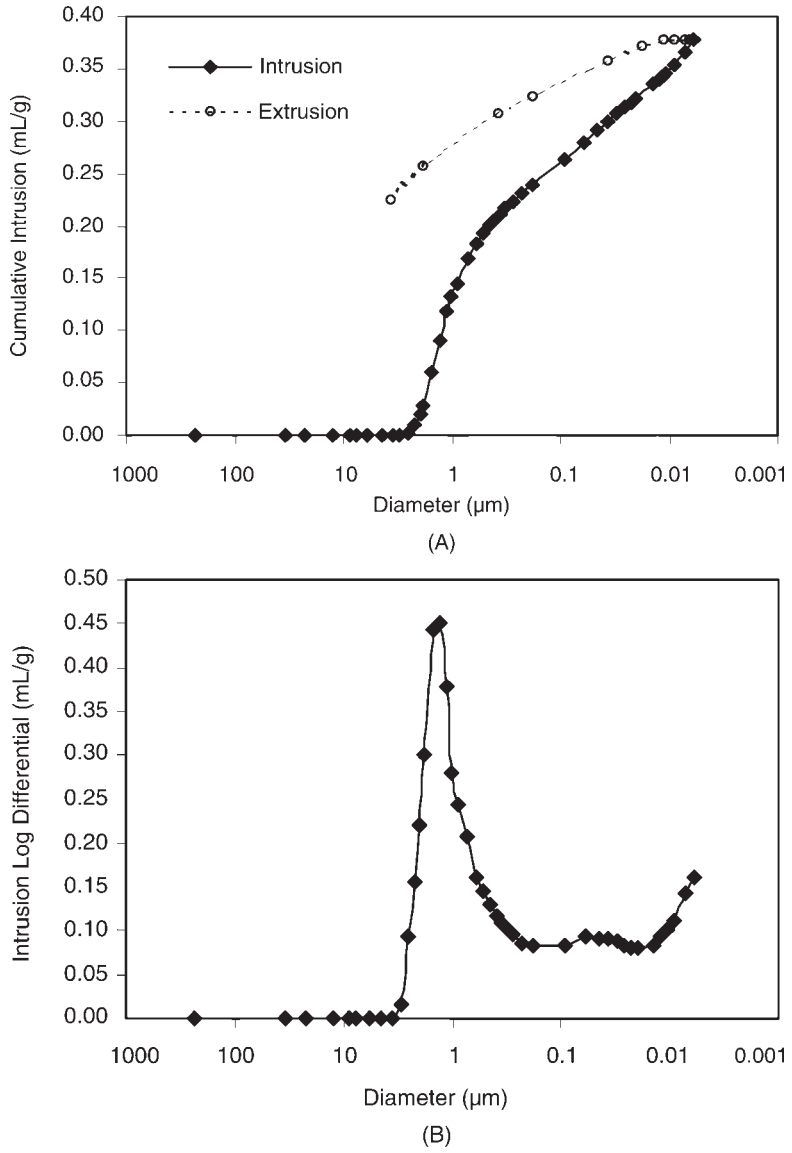

Figure 3. Pore-size distribution for MG50 obtained by mercury porosimetry (A) cumulative and (B) differential.

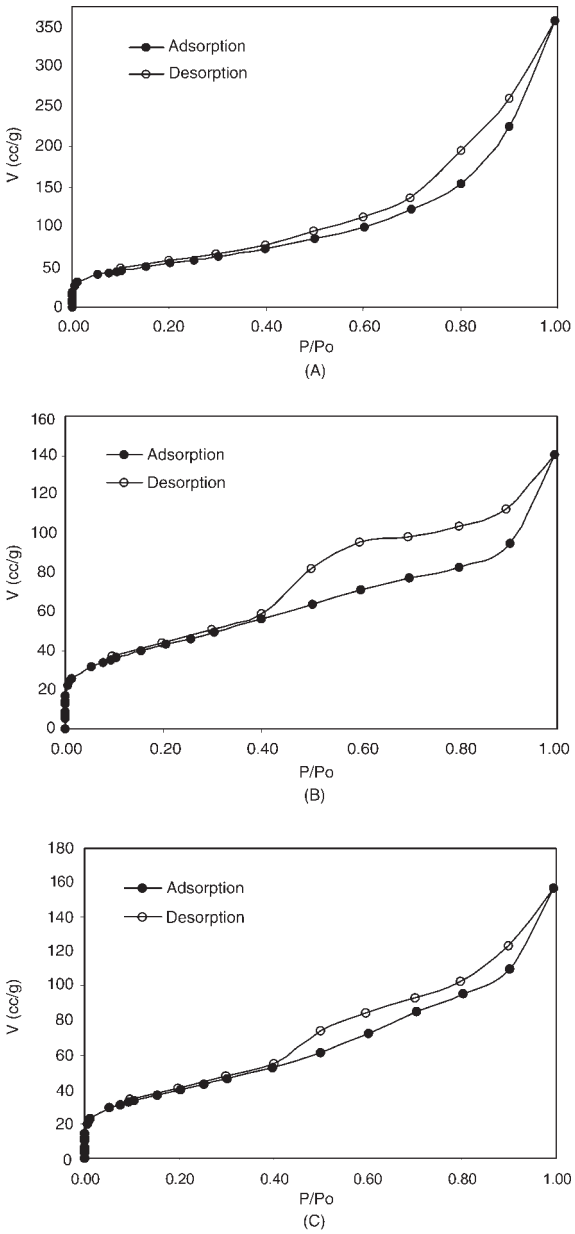

Figure 4. Isotherms of adsorption of N_2 at 77 K (A) MG 30; (B) MG 50; and (C) MG 70.

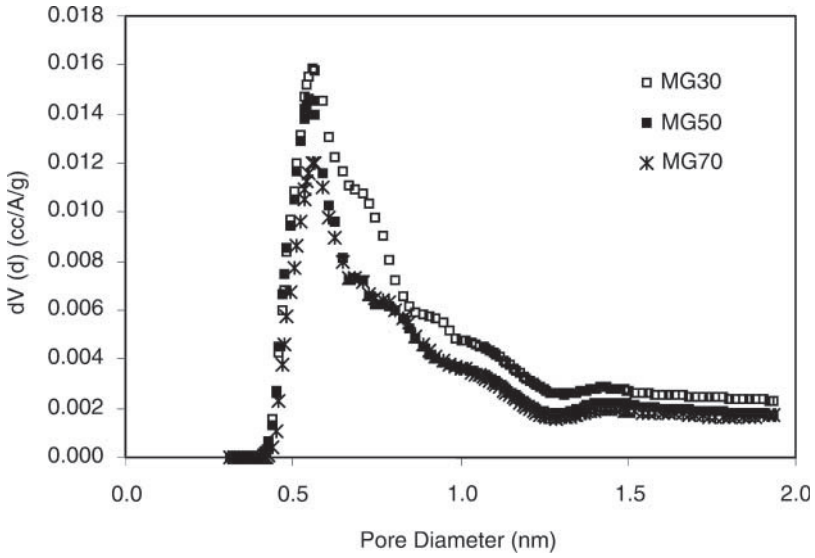

Figure 5. Micropore size distribution (HK plot).

A small quantity of pellets[1–3] of cylindrical shape, corresponding to a total mass of approximately 0.15 g, was placed in the cell of the ZLC apparatus. The ZLC cell had a length of 2.10 cm and an internal diameter of 0.44 cm. It was placed in a gas chromatograph oven (CG 35, Instrumentos Científicos), which also was used for the analysis of the exit gas by thermal conductivity detector.

The samples were previously treated by passing a flow of helium of 20 cm^3/min at 623 K (5 K/min heating ramp) for 2 hr and then keeping them for 2 hr more at the same temperature under vacuum (1.0 mbar). After this pretreatment, the hydrotalcite sample was saturated for 1 hr by passing a CO_2/He mixture (3% v/v; White and Martins). At this low CO_2 concentration, Henry's law describes the equilibrium of adsorption, as required by the ZLC model.[11–14] After saturation of the sample, desorption of CO_2 was carried out by using helium as the purge gas (99.995% purity, White and Martins) at 35, 50, and 70 cm^3/min (Figs. 7–10). The desorption curve was recorded until complete desorption of CO_2, and the results were analyzed to obtain the diffusivity of CO_2 onto hydrotalcites. The characteristics of the ZLC cell are summarized in Table 1.

The whole system was operated at the total pressure of 1.0 bar, and the experiments were carried out at 423, 523, and 623 K. Each experiment was reproduced at least three times.

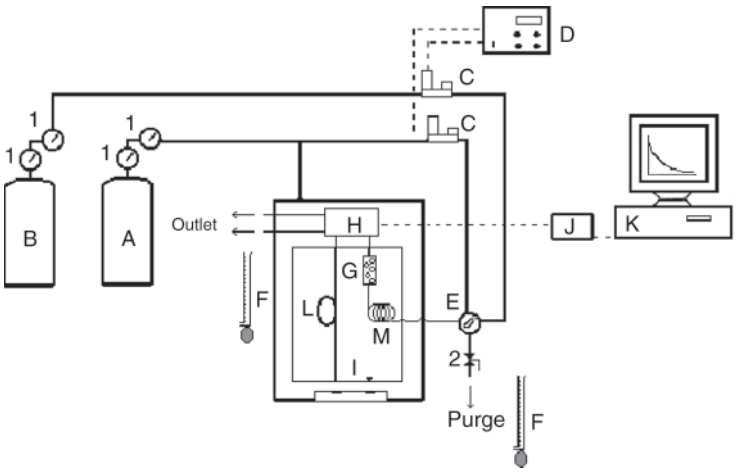

Figure 6. Schematic diagram of the experimental apparatus for measuring ZLC curves. *Key*: (A) helium gas bottle; (B) carbon dioxide gas bottle (3% CO_2 and 97% He); (C) mass flux control (MFC); (D) control unit of MFC; (E) four way valve; (F) film flowmeter; (G) ZLC cell; (H) TCD; (I) chromatograph oven; (J) data acquisition board of TCD; (K) computer; (L) reference gass (pure He); (M) preheater; (1) manometers; (2) valves.

Mathematical Models

The analysis of ZLC systems controlled by macropore or micropore diffusion is well documented in the literature.[10–19,24] The system is formally similar to the problem of diffusion with surface evaporation that is discussed by Crank.[25] By solving the Fickian diffusion equation, together with a mass balance over the cell and negligible fluid hold-up [24], the effluent concentration in the desorption step with micropore control[12] for slab geometry of the lamellar structures is:

$$\frac{C}{C_0} = 2L \sum_{n=1}^{\infty} \frac{\exp(-D_c \beta_n^2 t/l^2)}{\beta_n^2 + L(L+1)} \tag{1}$$

where C is the molar concentration of CO_2 in the gas phase (mol/m^3), C_0 is the initial molar concentration of CO_2 in the gas phase (mol/m^3), t is the time (sec) and β_n is given by the positive roots of the transcendental equation [Eq. (2)].

$$\beta_n \tan(\beta_n) = L \tag{2}$$

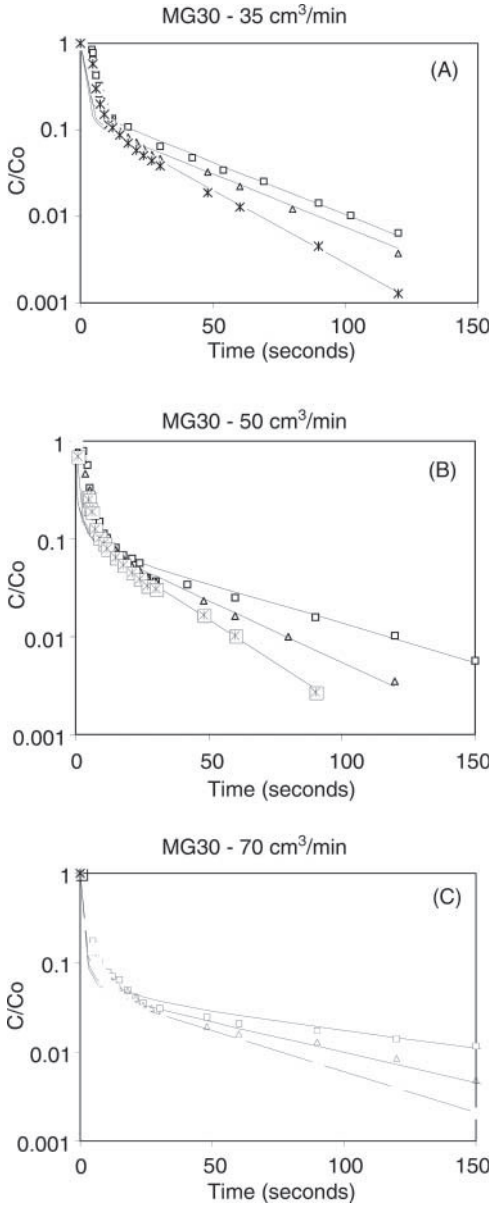

Figure 7. ZLC desorption curves and simulations with different flow rates of He as the inert purge gas at 423, 523, and 623 K in MG30: (A) 35 cm^3/min; (B) 50 cm^3/min; and (C) 70 cm^3/min. *Key*: (□) T = 423 K; (△) T = 523 K; (∗) T = 623 K.

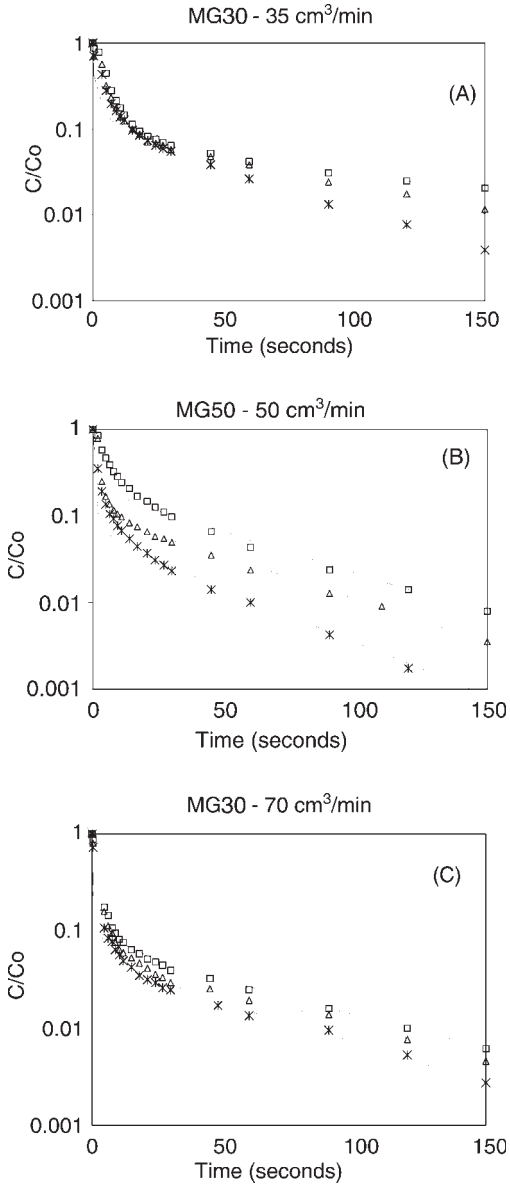

Figure 8. ZLC desorption curves and simulations with different flow rates of He as the inert purge gas at 423, 523, and 623 K in MG50: (A) 35 cm^3/min; (B) 50 cm^3/min; and (C) 70 cm^3/min. *Key*: (□) T = 423 K; (△) T = 523 K; (∗) T = 623 K.

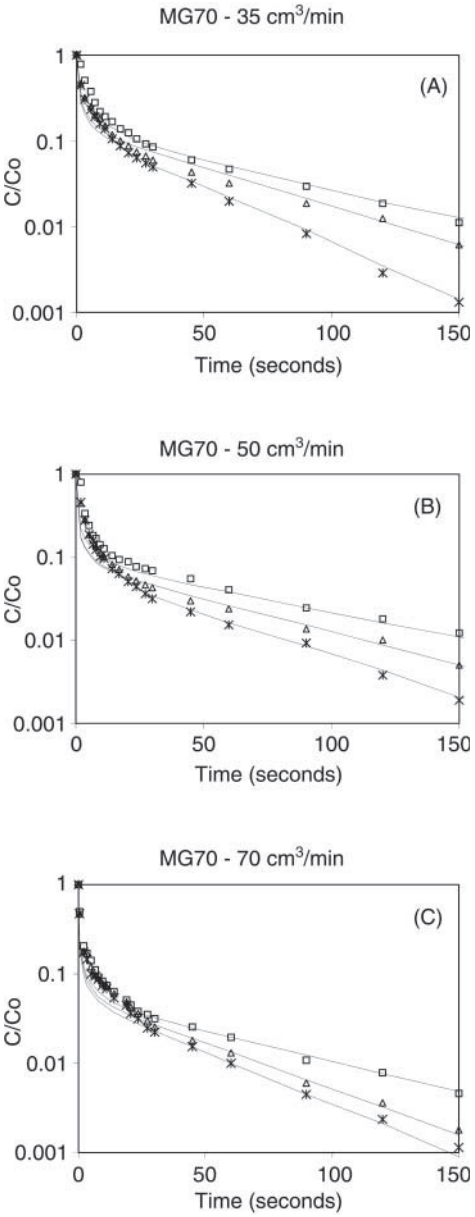

Figure 9. ZLC desorption curves and simulations with different flow rates of He as the inert purge gas at 423, 523, and 623 K in MG70: (A) 35 cm^3/min; (B) 50 cm^3/min; (C) 70 cm^3/min. *Key*: (□) T = 423 K; (△) T = 523 K; (∗) T = 623 K.

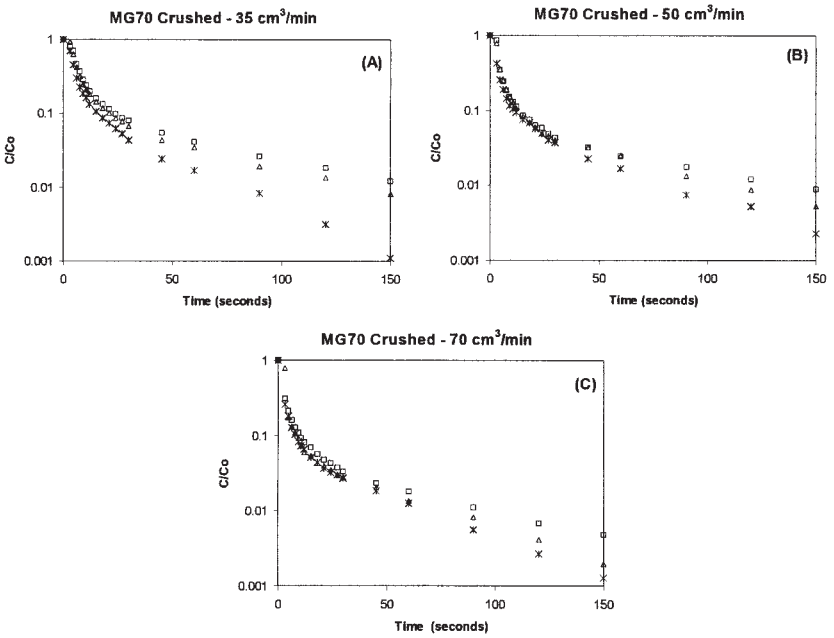

Figure 10. ZLC desorption curves with different flow rates of He at 423, 523, and 623 K in MG70 crushed: (A) 35 cm^3/min; (B) 50 cm^3/min; (C) 70 cm^3/min. *Key*: (□) T = 423 K; (△) T = 523 K; (∗) T = 623 K.

L is the ZLC parameter model, defined by Eq. (3).

$$L = \frac{Q_p l^2}{K V_s D_c} \tag{3}$$

where D_c is the micropore diffusivity (cm^2/sec), Q_p is purge flow rate (cm^3/min), l is the half-thickness of the adsorbent crystal (slab geometry) (cm), V_s is the solid volume inside the cell (cm^3), and K is the Henry constant.

Table 1. Characteristics of ZLC cell.

	MG30	MG50	MG70
Solid volume in cell (cm^3)	0.165	0.145	0.153
Cell volume (cm^3)	0.32	0.32	0.32
Solid mass in cell (g)	0.1463	0.1447	0.1953
Cell porosity	0.48	0.54	0.52

L may be interpreted as the ratio of characteristic diffusion time (l^2/D_c) to convection/adsorption time (V_sK/Q_p). A large value of L implies that micropore diffusion controls the rate at which the material is removed from the bed.[24]

For large values of time, Eq. (1) can be simplified and, thus, only the first terms of the series are significant, which provides a simpler graphical analysis: the long-time (LT) straight line on a semi-logarithmic scale is:[13,14,24]

$$\ln\left(\frac{C}{C_0}\right) = \ln\left[\frac{2\mathrm{L}}{\beta_1^2 + L(L+1)}\right] - \left(\frac{\beta_1^2 D_c}{l^2}\right)t \tag{4}$$

where the slope is given by $\beta_1^2 D_c/l^2$, the intercept is $\ln[2L/(\beta_1^2 + L(L+1))]$, and β_1 is the first root of transcendental Eq. (2).

All experiments were fitted to the complete model [Eqs. (1)–(3)] and with the LT response [Eq. (4)]. For the case where the complete model was used, in the region of LT only, we evaluated the experimental error by using the average of the residuals (ARE) given by Eq. (5):

$$\mathrm{ARE} = \frac{100}{S}\sum_{k=1}^{S}\left|\frac{(C/C_0)_{\mathrm{Calculated}} - (C/C_0)_{\mathrm{Experimental}}}{(C/C_0)_{\mathrm{Calculated}}}\right| \tag{5}$$

where S is the number of experimental points and ARE is the average residuals error (%).

The diffusion-controlling mechanism can be confirmed by the evaluation of $\gamma(1 + \mathrm{K})$, where γ is defined by Eq. (6). Crystal diffusivity is the controlling mechanism for $\gamma(1 + K) < 0.5$ in relation to the slab geometry model.[13]

$$\gamma = \frac{(D_c/l^2)}{(D_p/R_p^2)} \tag{6}$$

where R_p is the pellet radius (cm) and D_p is the pore diffusivity (cm), which is related to the Knudsen and molecular diffusion by the Bosanquet equation [Eq. (7)]

$$\frac{1}{D_p} = \tau_p\left(\frac{1}{D_m} + \frac{1}{D_K}\right) \tag{7}$$

D_m and D_K were evaluated according to the Chapman–Enskog and Knudsen equation (cm^2/sec), respectively, and τ_p is the tortuosity factor.[4]

The micropore controlling mechanism was experimentally detected in this work, performing runs with different pellet sizes.

Table 2. Characterization of Puralox adsorbents MG30, MG50, and MG70.

	MG30	MG50	MG70
Pellet geometry	Cylinder	Cylinder	Cylinder
$MgO : Al_2O_3$ (%)[a]	30 : 70	50 : 50	70 : 30
$MgO : Al_2O_3$ (%)[b]	28.5 : 71.5	46.7 : 53.3	63.5 : 36.5
Pellet length (cm)	0.46	0.45	0.45
Pellet diameter (cm)	0.39	0.37	0.38
Pellet volume (cm^3)	0.055	0.048	0.051
Solid humidity (%)	10.5	16.5	13.7
Solid density (g/cm^3)	2.45	3.07	2.80
Pellet density (g/cm^3)	0.88	1.13	0.91
Solid porosity	0.64	0.63	0.68
BET surface area (m^2/g)[c]	199.4	154.0	144.1
DR method micropore area (m^2/g)[c]	206.3	161.5	145.9
DR method micropore volume (cm^3/g)[c]	0.0733	0.0574	0.0519
HK method pore width (A)[c]	5.575	5.525	5.625

[a]Data obtained from Condea (SASOL) for the powdered samples.
[b]This work, from EDAX analysis.
[c]This work, from N_2 adsorption at 77 K.

RESULTS AND DISCUSSION

The adsorbent materials were characterized by using SEM/EDAX, mercury porosimetry, and N_2 adsorption at 77 K, where the presence of micropores is indicated. Table 2 shows the mean characterization values of Puralox adsorbents MG30, MG50, and MG70. The HK plot indicates values of pore width around 0.55 nm. The BET surface area and DR method micropore area have values of around 150 m^2/g.

For $\ln C/C_0$ vs. time t, the LT slope and intercept are calculated according to Eq. (4), and is shown in Table 3. Desorption curves for CO_2 from the hydrotalcite samples MG30, MG50, MG70 were measured by using flow rates of 30, 50, and 70 cm^3/min. The errors (ARE) also are presented.

To confirm that micropore diffusion was the controlling step, measurements were made with two different pellet sizes.[17] The results for the MG70 sample are shown in Table 4 with original and crushed pellets (1.55 mm). Little variation in the LT slope of the desorption curves was observed. For the micropore-controlled case, the solution was not influenced by the shape of the adsorbent pellet and we assumed slab geometry for the region containing the micropores. Table 5 shows the

Table 3. Linear coefficients for LT and error values for the hydrotalcite samples MG30 and MG50 at different flows.

	Sample					
	MG30			MG50		
T (K)	Slope (sec^{-1})	Intercept	ARE (%)	Slope (sec^{-1})	Intercept	ARE (%)
$Q_p = 35\,cm^3/min$						
423	−0.0278	−1.7842	5.7	−0.0119	−2.2818	9.8
523	−0.0282	−2.0684	7.7	−0.0155	−2.2349	9.2
623	−0.0388	−1.9843	7.1	−0.0235	−2.1368	6.9
$Q_p = 50\,cm^3/min$						
423	−0.0185	−2.4393	10.7	−0.0219	−1.6388	8.0
523	−0.0288	−2.3192	6.9	−0.0225	−2.2762	4.8
623	−0.0407	−2.1787	5.8	−0.0284	−2.8273	7.2
$Q_p = 70\,cm^3/min$						
423	−0.0093	−3.1238	9.8	−0.0192	−2.5173	5.1
523	−0.0155	−3.0675	10.8	−0.0157	−2.9598	4.8
623	−0.0212	−3.0037	6.5	−0.0193	−3.0181	7.7

values of the linear equilibrium constant (K) in the Henry's law region, for all flow rates and all the samples, obtained from the ZLC experiments. The value of K is an average of the results from three experiments at the same temperature and flow rate. The K values decrease when the temperature increases, and the heat of adsorption estimated is -6.21 ± 0.4; -7.28 ± 0.5, and $-5.60 \pm 1.0\,kJ\,mol^{-1}$ for MG30, MG50, and MG70, respectively. These low values indicate physical adsorption. The equilibrium constants shown in Table 5 are consistent with previous results reported by Soares et al.[30] and increase in the order MG50 > MG30 > MG70. The capacity of CO_2 adsorption of hydrotalcites depends on the aluminum content, which modifies their characteristics. As the aluminum content increases, the density of the layer charge increases and the number of high-strength sites for CO_2 adsorption decreases due to the decreasing of the interlayer spacing of hydrotalcites. This could explain why MG50 is the best adsorbent to CO_2.

Table 5 shows average D_c/l^2 values at temperatures 423–623 K, which are in the range $8.5 \times 10^{-3} - 15.3 \times 10^{-3}\,sec^{-1}$ for MG30, $8.0 \times 10^{-3} - 10.4 \times 10^{-3}\,sec^{-1}$ for MG50, and $6.8 \times 10^{-3} - 11.3 \times 10^{-3}\,sec^{-1}$ for MG70. These values are of the same order of magnitude as those found by Van Der Broeke and Krishna[28] and Rutherford and Coons[29] for the diffu-

Table 4. Linear coefficients for LT and error values for the hydrotalcite sample MG70 with original and crushed pellets at different flows.

	Sample				
	MG70 Original pellets			MG70 Crushed pellets[a]	
T (K)	Slope (sec^{-1})	Intercept	ARE (%)	Slope (sec^{-1})	Intercept
$Q_p = 35\,cm^3/min$					
423	−0.0177	−1.8885	8.5	−0.0176	−1.9863
523	−0.0194	−2.1467	12.1	−0.0196	−2.0274
623	−0.0312	−1.9935	6.8	−0.0316	−2.0735
$Q_p = 50\,cm^3/min$					
423	−0.0158	−2.1695	9.4	−0.0160	−2.5862
523	−0.0181	−2.6194	7.9	−0.0181	−2.5838
623	−0.0241	−2.6022	5.3	−0.0244	−2.4899
$Q_p = 70\,cm^3/min$					
423	−0.0171	−2.8828	3.2	−0.0175	−2.8357
523	−0.0241	−2.8050	7.0	−0.0242	−2.7686
623	−0.0268	−2.8989	6.3	−0.0262	−2.7733

[a]Solid mass in cell: 0.1515 g; solid volume in cell: 0.1665 cm^3; average pellet diameter: 0.155 cm; average pellet volume: 0.0025 cm^3; cell porosity: 0.48.

sion of CO_2 on other microporous materials where the controlling mechanism is the micropore diffusion.

The $\gamma(1 + K)$ values are also shown in Table 5. It can be observed that all values are lower than 0.5, confirming that the controlling mechanism is the micropore diffusion.

The Arrhenius dependence of the diffusivity resulted in activation energies for the diffusion of CO_2 on MG30, MG50, and MG70 of 6.2, 4.0, and 5.0 $kJ\,mol^{-1}$, respectively. These values are similar to the corresponding heat of adsorption, as were also reported by Van Den Broeke and Krishna[28] for the adsorption of CO_2 and CH_4 on microporous activated carbon.

The measurement of the adsorption equilibrium isotherms of CO_2 in extrudate samples of hydrotalcites MG30, MG50, and MG70 has been presented by Soares et al.[30] For MG50, the capacity of adsorption is 0.64 and 0.36 mmol/g at 423 and 723 K, respectively, at a pressure of 1.0 bar. The adsorption process is reversible and shows a reversal of the isotherms between 623 and 723 K.

Table 5. Average parameters K and D_c/l^2 for flows of 35, 50, and 70 cm^3/min for ZLC simulation by LT method for hydrotalcite samples MG30, MG50, and MG70.

T (K)	$K(-)$	$D_c/l^2 \times 10^3$ (sec^{-1})	$\gamma(1+K)$
MG30			
423	40.6 ± 1.6	8.5 ± 3.3	0.38
523	32.8 ± 1.8	10.9 ± 2.8	0.27
623	30.1 ± 1.9	15.3 ± 4.1	0.26
MG50			
423	46.6 ± 0.3	8.2 ± 1.9	0.42
523	40.2 ± 1.1	8.0 ± 1.5	0.24
623	39.1 ± 1.9	10.4 ± 1.5	0.23
MG70			
423	33.9 ± 3.2	6.8 ± 0.1	0.25
523	29.9 ± 0.8	9.3 ± 0.8	0.21
623	21.3 ± 1.9	11.3 ± 0.7	0.14

CONCLUSION

In this work, hydrotalcite materials are characterized by their textural structure and chemical composition. These adsorbents are essentially microporous, as shown by SEM/EDAX, mercury porosimetry, and N_2 adsorption at 77 K. The HK plot provided pore width values of about 0.55 nm. The BET surface area and DR-method micropore area were about 150 m^2/g. The diffusivity of CO_2 was obtained by the ZLC method for three hydrotalcite materials in the temperature range 423–623 K at three different flow rates: 30, 50, and 70 cm^3/min.

The values of the reciprocals of micropore diffusivity time constants (D_c/l^2) are in the range (8.5–15.3) $\times 10^{-3}$, (8.0–10.4) $\times 10^{-3}$, and (6.8–11.3) $\times 10^{-3}$ sec^{-1} for MG30, MG50, and MG70, respectively. The diffusion in the micropores is the controlling mechanism, and the dependence of D_c/l^2 can be described by Arrhenius equation with activation energies of 6.2, 4.0, and 5.0 $kJ\,mol^{-1}$ for MG30, MG50, and MG70, respectively.

NOMENCLATURE

ARE average of residuals error (%)

C	molar concentration of the sorbate in the gas phase (mol/m^3)
C_0	initial molar concentration of the sorbate in the gas phase (mol/m^3)
D_c	micropore diffusivity (cm^2/sec)
D_p	diffusivity in macropores (cm^2/sec)
D_K	Knudsen diffusion coefficient (cm^2/sec)
D_m	molecular diffusion coefficient (cm^2/sec)
K	equilibrium constant
l	half-thickness of the crystal (slab cm)
L	ZLC parameter defined by Eq. (3)
Q_p	purge flow rate (cm^3/min)
R_p	equivalent pellet radius (cm)
S	number of experimental points
t	time (sec)
T	temperature (K)
V_s	volume of adsorbent inside the ZLC cell (cm^3)

Greek Letters

β_1	first root of transcendental Eq. (2)
β_n	root of transcendental Eq. (2)
γ	ratio of micropore and macropore diffusional time constants ($\gamma = (D_c/l^2)/(D_p/R_p^2)$)
τ_p	tortuosity factor

ACKNOWLEDGMENTS

José L. Soares was a Ph.D. student supported by CNPq (Brazil) and Carlos A. Grande is a Ph.D. student at the LSRE, supported by the Foundation for Science and Technology (FCT-Portugal). This work is part of an on-going LSRE project "Adsorption-enhanced methane steam-reforming process for hydrogen production."

REFERENCES

1. Yong, Z.; Mata, V.; Rodrigues, A.E. Adsorption of carbon dioxide onto hydrotalcite-like compounds (Htlcs) at high temperatures. Ind. Eng. Chem. Res. **2001**, *4* (1), 204–209.
2. Yang, R.T.; Kikkinides, E.S.; Cho, S.H. Concentration and recovery of CO_2 from flue gas by pressure swing adsorption. Ind. Chem. Eng. Res. **1993**, *32* (11), 2714–2720.

3. Yong, Z.; Mata, V.; Rodrigues, A.E. Adsorption of carbon dioxide on chemically modified high surface area carbon-based adsorbents at high temperature. Adsorption **2001**, *7* (1), 41–50.
4. Ruthven, D.M. *Principles of Adsorption and Adsorption Processes*, 1st Ed.; John Wiley and Sons: New York, 1984.
5. Cavani, F.; Trifirò, F.; Vaccari, A. Hydrotalcite-type anionic clays: preparation, properties and applications. Catalysis Today **1991**, *11* (2), 173–301.
6. Kaneda, K.; Ueno, S.; Ebitani, K. Catalysis of layered hydrotalcites in heterogeneous hydrocarbon oxidations. Current Topic Catalysis **1997**, *1* (1), 91–105.
7. Velu, S.; Swamy, C.S. Kinetics of the alkylation of phenol with methanol over catalysts derived from hydrotalcite-like anionic clays. React. Kinet. Catal. Lett. **1997**, *62* (2), 339–346.
8. Ding, Y.; Alpay, E. Adsorption-enhanced steam reforming. Chem. Eng. Sci. **2000**, *55* (18), 3929–3940.
9. Ding, Y.; Alpay, E. Equilibria and kinetics of CO_2 adsorption on hydrotalcite adsorbent. Chem. Eng. Sci. **2000**, *55* (17), 3461–3474.
10. Hufton, J.R.; Ruthven, J.R. Diffusion of light alkanes in silicate studied by the zero length column method. Ind. Eng. Chem. Res. **1993**, *32* (10), 2379–2386.
11. Eic, M.; Ruthven, D.M. A new experimental technique for measurement of intracrystalline diffusivity. Zeolites **1988**, *8* (1), 40–45.
12. Brandani, S.; Ruthven, D.M. Analysis of ZLC desorption curves for gaseous systems. Adsorption **1996**, *2* (2), 133–143.
13. Grande, C.A.; Gigola, C.; Rodrigues, A.E. Adsorption of propane and propylene in pellets and crystals of 5A zeolite. Ind. Eng. Chem. Res. **2002**, *41* (1), 85–92.
14. Grande, C.A.; Rodrigues, A.E. Adsorption equilibria and kinetics of propane and propylene in silica gel. Ind. Eng. Chem. Res. **2001**, *40* (7), 1686–1693.
15. Silva, J.A.C.; Rodrigues, A.E. Analysis of ZLC technique for diffusivity measurements in bidisperse porous adsorbent pellets. Gas. Sep. Purif. **1996**, *10* (4), 207–224.
16. Silva, F.A.; Rodrigues, A.E. Adsorption equilibria and kinetics for propylene and propane over 13X and 4A zeolite pellets. Ind. Eng. Chem. Res. **1999**, *38* (5), 2051–2057.
17. Ruthven, D.M.; Xu, Z. Diffusion of oxygen and nitrogen in 5A zeolite crystals and commercial 5A pellets. Chem. Eng. Sci. **1993**, *48* (18), 3307–3312.

18. Han, M.; Yin, X.; Jin, Y.; Chen, S. Diffusion of aromatic hydrocarbon in ZSM-5 studied by the improved zero length column method. Ind. Eng. Chem. Res. **1999**, *38* (8), 3172–3175.
19. Brandani, S. Analytical solution for ZLC desorption curves with bi-porous adsorbent particles. Chem. Eng. Sci. **1996**, *51* (12), 3283–3288.
20. Brunauer, S.; Deming, L.S.; Deming, W.S.; Teller, E. On a theory of the Van der Waals adsorption of gases. J. Am. Chem. Soc. **1940**, *62* (7), 1723–1732.
21. Horváth, G.; Kawazoe, K. Method for calculation of effective pore size distribution in molecular sieve carbon. J. Chem. Eng. Jpn **1983**, *16* (6), 470–475.
22. Yong, Z.; Rodrigues, A.E. Hydrotalcite-like compounds as adsorbents for carbon dioxide. Energ. Conv. Manang. **2002**, *43* (14), 1865–1876.
23. Mckenzie, A.L.; Fischel, C.T.; Davis, R.J. Investigation of the surface structure and basic properties of calcined hydrotalcites. J. Catal. **1992**, *138* (2), 547–561.
24. Duncan, W.L.; Moller, K.P. A 'zero length criterion' for ZLC chromatography. Chem. Eng. Sci. **2000**, *55* (22), 5415–5420.
25. Crank, J. *The Mathematics of Diffusion*, 2nd Ed.; Clarendon Press: Oxford, 1975.
26. Cavalcante, C.L., Jr.; Brandani, S.; Ruthven, D.M. Evaluation of the main diffusion path in zeolites from ZLC desorption curves. Zeolites **1997**, *18* (4), 282–285.
27. Soares, J.L. *Desenvolvimento de Novos Adsorventes e Processos Híbridos em Reforma Catalítica por Vapor de Água*; Tese de Doutorado; UFSC: Florianópolis/SC, Brazil, 2003.
28. Van Der Broeke, L.J.P.; Krishna, R. Experimental verification of the Maxwell–Stephan theory for micropore diffusion. Chem. Eng. Sci. **1995**, *50* (16), 2507–2522.
29. Rutherford, S.W.; Coons, J.E. Adsorption dynamics of carbon dioxide in molecular sieving. Carbon **2003**, *41* (3), 405–411.
30. Soares, J.L.; Grande, C.A.; Yong, Z.; Moreira, R.F.P.M.; Rodrigues, A.E. *Adsorption of Carbon Dioxide at High Temperatures onto Hydrotalcite-like Compounds (HTlcs)*. Proceeedings of Fundamentals of Adsorption 7, Chiba-City, Japan, 2002; Kaneko, K., Kanoh, H., Hanzawa, Y., Eds.; IK International Ltd, 2002.